Cureus Journal of Engineering

Open Access Original Article

Integrating Multi-Criteria Decision-Making and the Taguchi Method for High-Performance Material Selection in Rigid Flange Coupling Systems

Manoj M. Dongare [1] , Swapnil S. Bhoir [1] , Munna Verma [1]

1. Department of Mechanical Engineering, Bhagwant University, Ajmer, IND

Corresponding author: Manoj M. Dongare, manoj1dongare@gmail.com

Received 03/13/2025
Review began 05/11/2025
Review ended 06/12/2025
Published 06/20/2025

DOI: https://doi.org/10.7759/s44388-025-03722-w

Abstract

Rigid flange couplings are essential components in mechanical power transmission systems, providing high torque transfer efficiency and structural integrity. The selection of optimal material combinations for these couplings is critical to ensuring durability, mechanical performance, and cost-effectiveness. This study presents a Multi-Criteria Decision-Making (MCDM) approach integrated with the Taguchi method and Finite Element Analysis (FEA) for systematic material selection and performance optimization.

The research methodology involved determining coupling dimensions through manual calculations, developing 3D models in SolidWorks, and performing FEA simulations under predefined boundary conditions. The Taguchi L9 orthogonal array was employed to identify the best-performing material combinations based on multiple performance criteria, including tensile strength, shear strength, compressive strength, fatigue resistance, density, cost, and manufacturability. Statistical validation techniques such as Signal-to-Noise (S/N) ratio analysis were applied to ensure the reliability of results and predictive accuracy.

Key findings indicate that integrating MCDM with the Taguchi method significantly enhances decision-making by balancing mechanical performance and economic feasibility. The optimized material selection improves equivalent stress distribution, shear stress resistance, total deformation, and equivalent elastic strain characteristics. This study bridges existing research gaps by offering a comprehensive, statistically validated, and experimentally optimized framework, benefiting engineers and industries involved in power transmission applications.

Categories: Advanced Manufacturing Technologies, Materials Engineering, Design and Manufacturing
Keywords: taguchi, finite element analysis, material optimization, mechanical performance, stress analysis

Introduction

Rigid flange couplings are critical in industrial power transmission systems, enabling the reliable transfer of torque between aligned shafts while maintaining high torsional rigidity. However, this rigidity introduces stress concentrations, necessitating material optimization to ensure durability under high torque, cyclic loading, and fluctuating operational conditions. Traditional material selection methods often overlook the integration of mechanical, economic, and manufacturability criteria, which are essential for achieving an optimal balance [1,2]. This study proposes a combined approach using Multi-Criteria Decision-Making (MCDM) techniques, the Taguchi method, and Finite Element Analysis (FEA) to address these limitations. MCDM enables a structured evaluation of key material properties, while the Taguchi method reduces simulation complexity by optimizing performance configurations through systematic testing. FEA complements these methods by simulating stress distributions and identifying critical stress zones, ensuring the robustness of material choices. This integrated framework not only enhances the performance and cost-effectiveness of rigid flange couplings but also offers a scalable solution for complex engineering applications [3,4].

The primary material requirements include:

How to cite this article
Dongare M M, Bhoir S S, Verma M (June 20, 2025) Integrating Multi-Criteria Decision-Making and the Taguchi Method for High-Performance Material Selection in Rigid Flange Coupling Systems. Cureus J Eng 2 : es44388-025-03722-w. DOI https://doi.org/10.7759/s44388-025-03722-w

Component	Key Material Requirements
Shaft	High tensile strength, fatigue resistance, shear strength
Flange	High compressive strength, shear strength, fatigue resistance
Key	Shear strength, toughness, fatigue resistance
Bolt	Tensile strength, fatigue resistance, cost-effectiveness

TABLE 1: Outlines key material requirements for each component of the coupling

Figure 1 shows the components of rigid flange couplings and Table 1 indicates several crucial mechanical properties. Tensile strength is essential for components like the shaft and bolts, which endure axial loads. Compressive strength is vital for flanges that experience compressive forces under torque. Shear strength is critical for keys and flanges to resist tangential forces and maintain alignment. Finally, fatigue resistance is necessary for all components to withstand cyclic stresses over time.

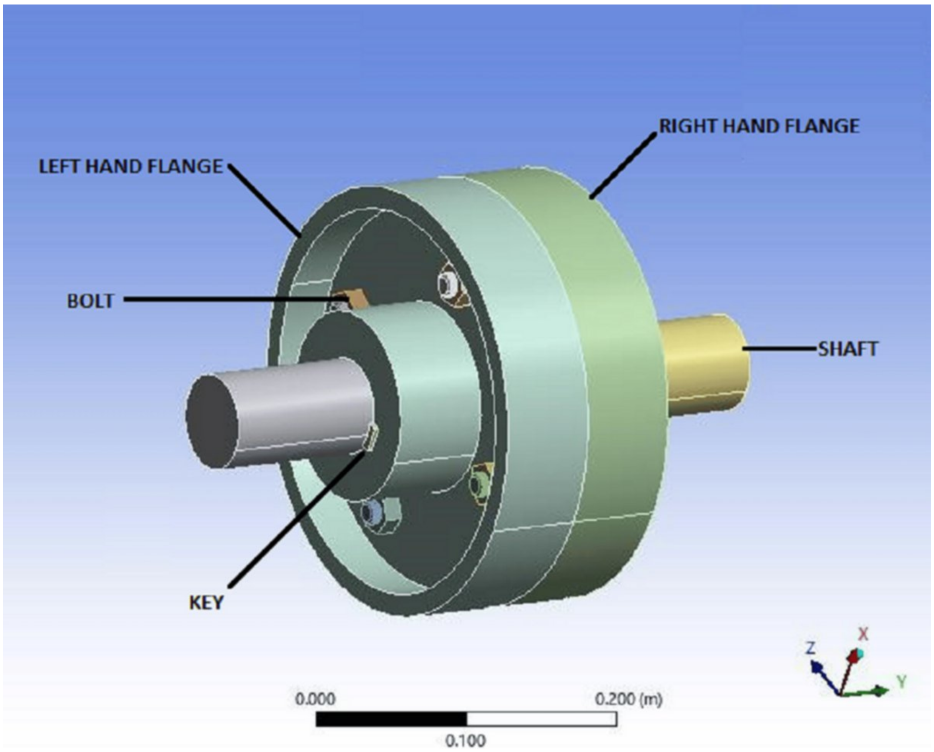

FIGURE 1: Rigid flange coupling

Traditional material selection methods for couplings have been largely empirical, relying on trial-and-error testing, which are time-consuming, costly, and mostly do not consider all relevant criteria's.

A structured evaluation of all relevant material properties are not considered in traditional material selection approaches. Conventional methods rarely integrate mechanical and economic criteria, such as manufacturability and cost, along with tensile strength and fatigue resistance. The interactions between properties, such as materials with high tensile strength, may reveal poor machinability, which make them costly and challenging to manufacture [5]. An optimized balance can be achieved by integration of computational simulations with statistical and multi-criteria decision-making methods. When multiple objectives must be balanced, MCDM techniques are widely recognized for their ability to facilitate complex decision-making in engineering design. For rigid flange couplings, MCDM enables a balanced evaluation across critical criteria, such as tensile strength, compressive strength, shear strength, and fatigue resistance, prioritizing each according to application-specific needs as well as cost and manufacturability can be integrated alongside technical criteria. It ensures that the selected materials are not only high-performing but also cost-effective and readily available [6,7].

In material optimization, the Taguchi method systematically select material combinations across multiple levels, ensuring a reduction in computational runs and to make valid conclusions from data. In the context of coupling design, the Taguchi method can be applied to test a range of material grades and optimize performance by identifying configurations that yield the highest mechanical performance with the least variability [8]. Engineers can systematically narrow down material options based on robust computational data by combining Taguchi's efficiency with MCDM's comprehensive evaluation. The Taguchi orthogonal array significantly streamlined the testing process. In material optimization for rigid flange couplings, engineers can predict stress distribution, deformation, and potential failure points by using FEA [9].

By integrating FEA with MCDM and the Taguchi method, this study leverages simulation-driven data to quantify the impact of each material on stress and strain distribution within the coupling also to identify areas of high stress concentration and validate computational findings from the Taguchi method. This combined approach not only provides a scalable model for other complex engineering applications but also addresses the limitations of traditional methods.

Literature review

Over the past decade, significant research efforts have been directed toward enhancing the design and operational effectiveness of flange couplings within demanding environments characterized by substantial loads and pressures. Numerous investigations have contributed to the field through the development of advanced modeling and optimization methodologies. Figure *2* shows the graphical representation of flow of the literature review.

Finite Element Analysis (FEA) and Structural Integrity

FEA has been widely employed to evaluate the stress distribution and deformation behavior of flange couplings under various loading conditions. Han utilized ANSYS Workbench for modal analysis of thrust coupling, confirming the efficiency of simulation-based approaches in predicting dynamic characteristics [1]. Hassan and Ali investigated the effects of misalignment on a rotating system using both simulation and computational methods, highlighting the critical impact of misalignment on mechanical performance [2]. Ji and Lu proposed a differential evolution algorithm for optimizing flange coupling designs through ANSYS simulations, demonstrating its reliability in enhancing structural performance [3]. Additionally, Li et al. explored active control strategies for rigid-flexible coupling in piezoelectric thin plates, emphasizing the role of intelligent materials in improving mechanical efficiency [4]. Mehmanparast et al. reviewed bolted flange connections in offshore wind applications, outlining the challenges associated with stress concentration and fatigue failure [5]. Moreover, Negishi et al. conducted fluid-rigid body coupling simulations using a physically consistent particle method, providing valuable insights into the complex interactions within coupled mechanical systems [6]. While these studies confirm the accuracy of numerical simulation techniques, most focus primarily on stress analysis and neglect the implementation of multi-objective optimization frameworks.

Material Selection and Performance Evaluation

The choice of materials significantly influences the structural integrity and performance of flange couplings. Patil et al. introduced an integrated design framework using Python scripting for parametric Computer-Aided Design modeling of flange couplings, facilitating systematic material selection and optimization [7]. Peng et al. developed a rigid-flexible-soft coupling dynamic model for clustered tensegrity structures, demonstrating the advantages of advanced material combinations in enhancing mechanical behavior [8]. Qu et al. further explored rigid-flexible coupling dynamics in robotic manta systems, providing evidence of how flexible materials improve structural adaptability [9]. Wang et al. analyzed a misaligned rigid rotor system with flexible supports, reinforcing the importance of material selection in mitigating misalignment-induced failures [10]. Despite these advancements, most studies examine individual materials without employing structured computational designs, such as the Taguchi L9 orthogonal array, to systematically evaluate multiple material configurations.

Optimization Techniques for Enhanced Performance

Optimization methodologies have been applied to enhance the design and operational efficiency of flange couplings. Bhoir et al. conducted an computational analysis of clearance between punch and die in sheet metal blanking, underlining the significance of process optimization in mechanical systems [11]. Dongare et al. reviewed various optimization techniques utilized in sheet metal blanking processes, advocating for the adoption of structured design approaches in mechanical engineering applications. Furthermore, Dongare et al. performed a comparative analysis of flange coupling models using different materials in a 3D printing , emphasizing the role of material optimization in additive manufacturing . While these studies highlight the benefits of optimization, there is a lack of predictive modeling approaches, such as regression and machine learning, to forecast mechanical behavior under different material and load conditions. Additionally, computational validation of FEA results remains scarce, limiting the practical applicability of simulation-based findings.

Research Gaps and Future Directions

Despite extensive research, several gaps persist in the current literature. Most studies primarily focus on stress analysis without integrating multi-objective optimization frameworks. A systematic approach to material selection, particularly through structured computational designs like the Taguchi L9 orthogonal array, remains underexplored. Predictive modeling techniques, including regression and machine learning, are largely absent, restricting the ability to accurately forecast stress distribution and deformation under varying conditions. Moreover, limited computational validation of FEA results reduces the reliability of numerical simulations. To address these gaps, this research will employ a systematic analysis of material combinations, conduct detailed FEA simulations, and validate results using ANOVA, regression, and predictive modeling, ultimately establishing a comprehensive and computationally validated design framework for rigid flange couplings.

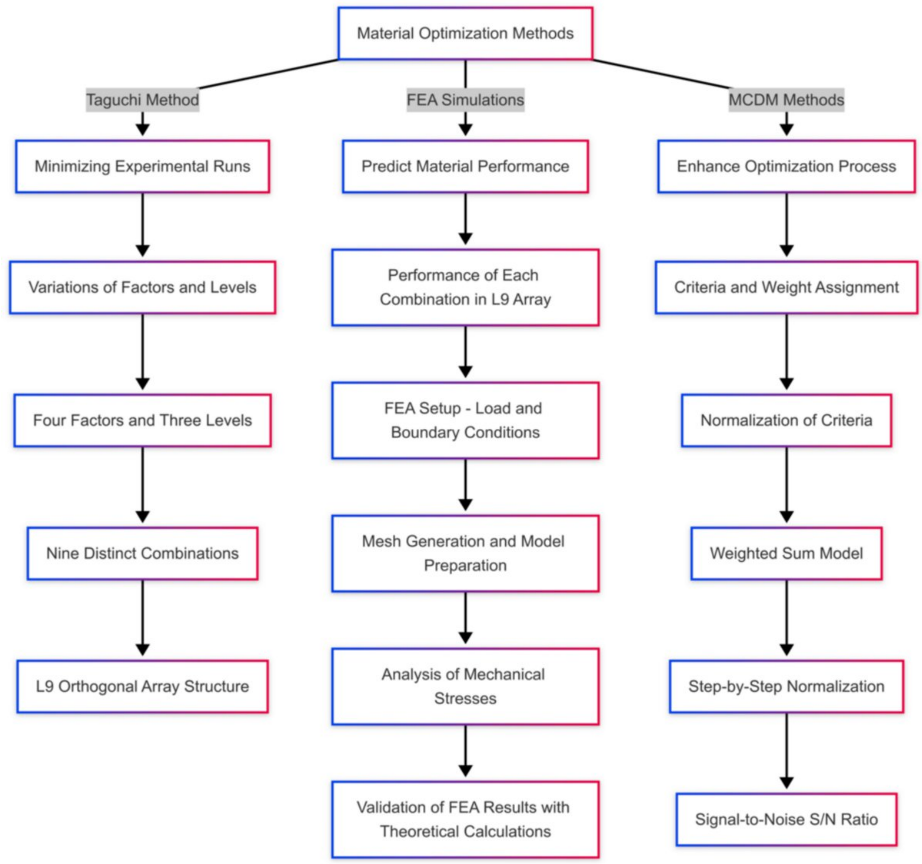

FIGURE 2: Graphical representation of flow of the literature review

FEA, Finite Element Analysis; MCDM, Multi-Criteria Decision-Making; S/N, Signal-to-Noise

Materials And Methods

Methodology

In a multi-phase approach, Figure *3* shows the methodology combines FEA simulations, MCDM, and the Taguchi method:

Phase 1: Selection and Structuring of Criteria for Material Optimization

Balancing mechanical performance with economic feasibility is crucial for selection and structuring of criteria in material optimization. The seven core criteria's were identified in this study: tensile strength, shear strength, compressive strength, fatigue resistance, density, cost, and manufacturability. It ensures that criteria's were chosen to meet the performance requirements for high-torque applications of rigid flange coupling components along with consideration of production constraints and economic viability.

Phase 2: Computational Design Using the Taguchi L9 Orthogonal Array

To aim minimum variability and maximum performance across multiple criteria, a structured approach is selected for optimizing parameters in material which can be provided by the Taguchi method. For reducing the required number of computational runs and complex combinations of material properties, the L9 array was selected. To evaluate various material combinations for rigid flange couplings, the Taguchi L9 orthogonal array is employed .

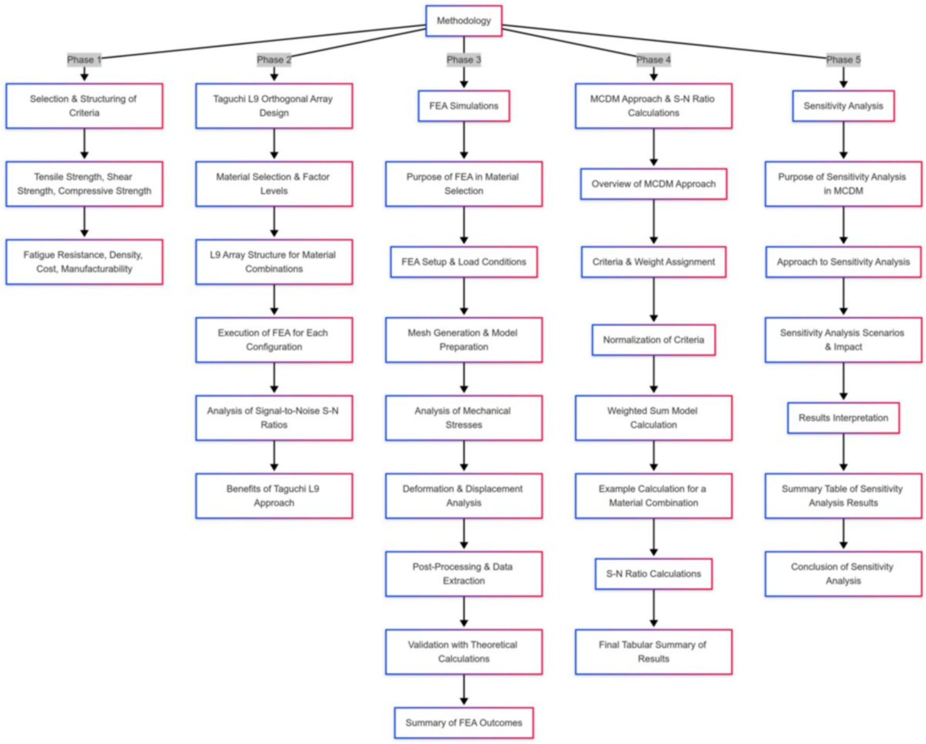

FIGURE 3: The methodology combines FEA simulations, MCDM, and the Taguchi method

FEA, Finite Element Analysis; MCDM, Multi-Criteria Decision-Making; S/N, Signal-to-Noise

Phase 3: Finite Element Analysis (FEA) Simulations

FEA is an essential tool in this study, providing insights into how different material combinations respond under operational conditions typical of rigid flange couplings. FEA simulations enable a detailed evaluation of each material configuration's mechanical performance, including its resistance to tensile, compressive, and shear stresses, which are critical in assessing durability and structural integrity.

Phase 4: Multi-Criteria Decision-Making (MCDM) Approach and S/N Ratio Calculations

In this phase, a MCDM approach was employed to evaluate and rank each material combination based on multiple performance criteria, including tensile stress, compressive stress, shear stress, and deformation. The goal was to identify the material combination that optimally balances these mechanical properties while minimizing stress levels, ensuring robustness under operational conditions.

Phase 5: Sensitivity Analysis Scenarios for Material Selection

In this section, we will cover all scenarios that might affect the material selection process when the weightings for different criteria change. Each scenario emphasizes different criteria to observe how sensitive the material selection is to changes in priorities. We will examine four different scenarios, in addition to the original weighting scheme, and analyze how the changes in weightings impact the composite score. The goal is to determine whether the material remains optimal under variable weighting conditions or if alternative materials should be considered under different priorities.

Material selection and safety considerations for rigid flange coupling design

The rigid flange coupling is designed with a focus on mechanical strength, durability, and manufacturability. Plain carbon steel is selected for the shafts, keys, and bolts due to its adequate torsional and compressive strength, applying a factor of safety (FOS) of 2.5. Gray cast iron is chosen for the flanges, leveraging its suitability for casting and applying an FOS of 2.5, with shear strength considered as half its tensile strength, ensuring safe performance under varying loads [12].

Permissible Stresses

Ductile materials, particularly carbon steels, are preferred for shafts due to their high strength and durability. A FOS of 2.5 is considered to ensure reliable performance under torsional loads. The maximum permissible shear stress (τmax) for different grades of carbon steel is determined based on their yield stress (σyt), as shown in the following Table *2*, which was used in the computation. This approach ensures that the selected shaft material can withstand operational stresses while maintaining structural integrity.

Sr. No.	Carbon Steel Grade	Yield Stress (σyt) (N/mm²)	Shear Stress (τmax) (N/mm²)
1	C07	196	39.2
2	C10	206	41.2
3	C15	235	47
4	C25	275	55
5	C35	304	60.8
6	C40	324	64.8
7	C45	353	70.6
8	C50	373	74.6
9	C60	412	82.4
10	C65	422	84.4

TABLE 2: Determining the value of shear stress for shaft

Gray cast iron is commonly used for flanges due to its excellent castability and high compressive strength. A FOS of 2.5 is applied to ensure the flange can withstand operational loads without failure. The maximum permissible shear stress (τmax) is determined as half of the ultimate tensile strength (σut) for various grades of gray cast iron. Table *3* presents the permissible shear stress values corresponding to different grades of gray cast iron used in the computation, ensuring the material selection meets both strength and safety requirements.

Sr. No.	Gray Cast Iron Grade	Ultimate Stress (σut) (N/mm²)	Shear Stress (τmax) (N/mm²)
1	FG150	150	30
2	FG200	200	40
3	FG220	220	44
4	FG260	260	52
5	FG300	300	60
6	FG350	350	70
7	FG400	400	80

TABLE 3: Determining the value of shear stress for flange

Keys and bolts are typically made from ductile materials, with carbon steels being the preferred choice due to their high strength and durability. A FOS of 2.5 is considered to ensure reliable performance under shear and compressive stresses. The maximum permissible shear stress (τmax) and permissible compressive stress (σc) are determined based on the yield stress (σyt) of different grades of carbon steel.

Table 4 presents these values, ensuring that the selected materials provide adequate strength and safety under operational conditions.

Sr. No.	Carbon Steel Grade	Yield Stress (σyt) (N/mm²)	Shear Stress (τmax) (N/mm²)	Compressive Stress (σc) (N/mm²)
1	C07	196	39.2	117.6
2	C10	206	41.2	123.6
3	C15	235	47	141
4	C25	275	55	165
5	C35	304	60.8	182.4
6	C40	324	64.8	194.4
7	C45	353	70.6	211.8
8	C50	373	74.6	223.8
9	C60	412	82.4	253.2
10	C65	422	84.4	253.2

TABLE 4: Determining the shear and compressive stresses for keys and bolts

The shaft diameter is determined by considering a service factor of 1.5. To ensure structural integrity, different shaft diameters are calculated based on the permissible shear stress (τ) of various carbon steel grades. After evaluating strength requirements and cost-effectiveness, C35 carbon steel is selected as the optimal material. The corresponding shaft diameter for the coupling design is 64 mm, ensuring it can safely transmit the required torque while maintaining durability and efficiency. Table 5 shows the design specification of coupling.

The selection of C60 for the shaft, FG300 for the flange, C45 for the key, and C35 for the bolt using the MCDM approach offers a comprehensive, balanced solution for high-performance mechanical applications, particularly in high-torque scenarios such as industrial couplings. The material combination addresses several key performance aspects, including mechanical strength, cost efficiency, and manufacturability.

Part Specification	Dimensions (mm)
Hub Diameter (dh)	2d = 2(60) = 120 mm
Hub Length (lh)	1.5d = 1.5(60) = 90 mm
Bolt Circle Diameter (D)	3d = 3(60) = 180 mm
Flange Thickness (t)	0.5d = 0.5(60) = 30 mm
Web Thickness (t1)	0.25d = 0.25(60) = 15 mm
Diameter of Spigot and Recess (dr)	1.5d = 1.5(60) = 90 mm
Outside Diameter of Flange (Do)	(4d + 2t1) = (4 × 60 + 2 × 15) = 270 mm

TABLE 5: Design specification of coupling

To validate the FEA results, stress values obtained from simulations were compared with those derived from analytical calculations. Manual calculations were performed using standard mechanical design equations for shear and compressive stresses on components like shafts, keys, bolts, and flanges.

The L9 orthogonal array is a well-structured Taguchi design of computation (DOE) method used for optimizing multiple factors with a minimal number of computational trials. In this study, the selection of shaft material, flange material, key material, and bolt material influences the performance of the rigid flange coupling. The justification for using the L9 array is as follows:

Efficient Material Optimization: Instead of testing all possible material combinations, which would be computationally expensive and time-consuming, the L9 array allows for an optimal selection of nine representative combinations to achieve significant insights into material performance.

Four Factors at Three Levels Each: The study considers four critical components (shaft, flange, key, and bolt materials), each with three different material choices. A full factorial approach would require $3^4 = 81$ trials, whereas L9 reduces it to just 9 trials, making the analysis more feasible.

Comprehensive Evaluation: The three material levels for each component provide a balanced assessment of material properties such as shear strength, compressive strength, fatigue resistance, and cost-effectiveness. The selected materials C35, C45, C60 for the shaft, FG200, FG260, FG300 for the flange, C35, C45, C60 for the key, and C35, C45, C60 for the bolt cover a wide range of mechanical properties.

Orthogonality for Statistical Significance: The orthogonal nature of the L9 array ensures that the effects of different material combinations are independently evaluated, improving the reliability of results. It enables signal-to-noise (S/N) ratio analysis, identifying the optimal combination that minimizes deformation while maximizing strength.

Taguchi's "Smaller-the-Better" Criterion: Since coupling deformations and stress variations need to be minimized, Taguchi's "smaller-the-better" approach is applied to analyze the impact of different materials and find the most robust combination.

Industrial Relevance and Practical Implementation: The materials selected align with industry standards for flange coupling design, ensuring practical applicability in real-world engineering applications.

Results

Taguchi L9 orthogonal array and its efficiency

The Taguchi L9 orthogonal array provides a powerful and efficient framework for investigating the influence of material selection on a system comprising a shaft, flange, key, and bolt. With four components, each having three potential material grades (carbon steels C35, C45, C60, and gray cast irons FG200, FG260, FG300), a full factorial design would necessitate 81 combinations. However, the L9 array strategically reduces this to just nine, significantly minimizing combinations effort while preserving statistical validity. This array meticulously assigns specific combinations of material grades to each of the nine combinations, ensuring a balanced and independent assessment of each component's impact on the overall system performance. By systematically varying the material properties across these carefully curated combinations, the L9 array allows for the identification of optimal material selections and the determination of each component's individual contribution to the system's behavior. Table 6 summarizes the material configurations used in the L9 array for this study:

Sr. No.	Shaft Material	Flange Material	Key Material	Bolt Material
1	C35	FG200	C35	C35
2	C35	FG260	C45	C45
3	C35	FG300	C60	C60
4	C45	FG200	C45	C60
5	C45	FG260	C60	C35
6	C45	FG300	C35	C45
7	C60	FG200	C60	C45
8	C60	FG260	C35	C60
9	C60	FG300	C45	C35

TABLE 6: Summarizes the material configurations used in the L9 array for this study

Structuring the criteria with weight assignments

In the material selection process for a high-torque industrial flange coupling, a MCDM framework is employed to systematically evaluate and prioritize various performance and economic factors. The relative importance of each criterion is quantified through assigned weights, reflecting the operational demands of the coupling. Recognizing the critical role of mechanical integrity, tensile strength, shear strength, compressive strength, and fatigue resistance are allocated substantial weights, emphasizing durability and reliability.

Criterion	Weight (%)
Tensile Strength	20
Shear Strength	20
Compressive Strength	15
Fatigue Resistance	20
Density	5
Cost	10
Manufacturability	10

TABLE 7: The original weighting scheme for the criteria

Balancing performance with cost-effectiveness, cost and manufacturability receive moderate weights. Given the application's emphasis on strength over weight reduction, density is assigned a lower weight. This structured approach, exemplified by the provided percentage-based weight distribution, enables a comprehensive evaluation, ensuring that the chosen materials not only meet stringent mechanical requirements but also remain economically viable and readily manufacturable. Table *7* indicates original weighting scheme for the criteria.

Finite Element Analysis (FEA) simulations

FEA is employed to assess the structural integrity of a rigid flange coupling, specifically evaluating the mechanical behavior of diverse material combinations. A three-dimensional (3D) geometric model of the coupling, as depicted in Figure *4*, serves as the basis for the analysis. Imposition of boundary conditions, as outlined in Table *8*, facilitates the generation of a discretized mesh, illustrated in Figure *5*. Subsequent simulation of operational loading conditions enables the determination of stress distribution patterns, identification of stress concentration regions, and quantification of deformation magnitudes under applied torsional loads.

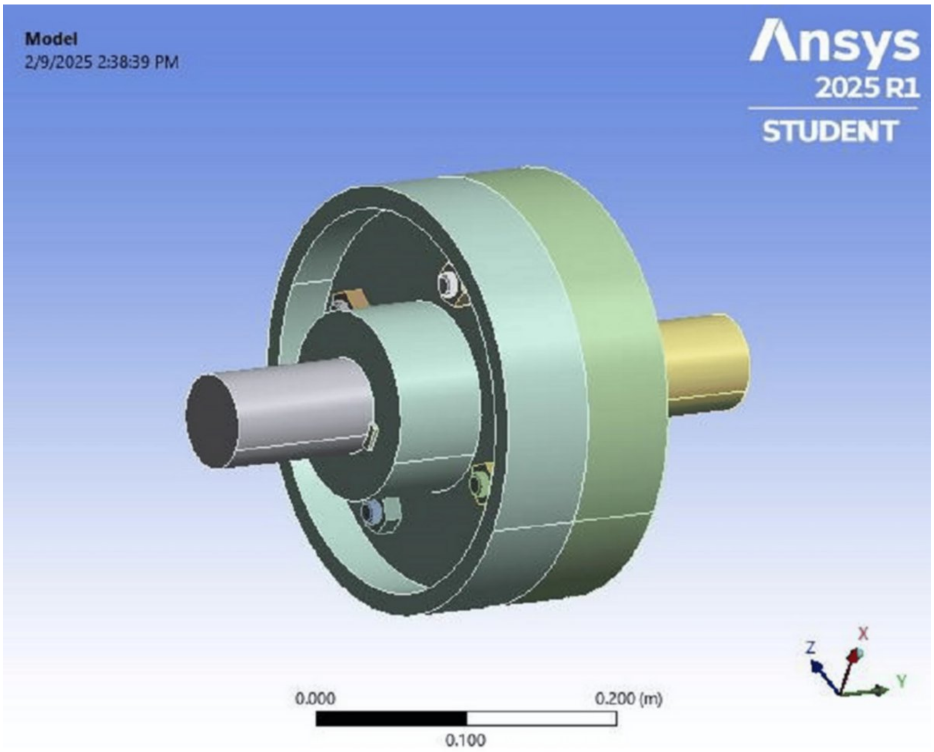

FIGURE 4: 3D model

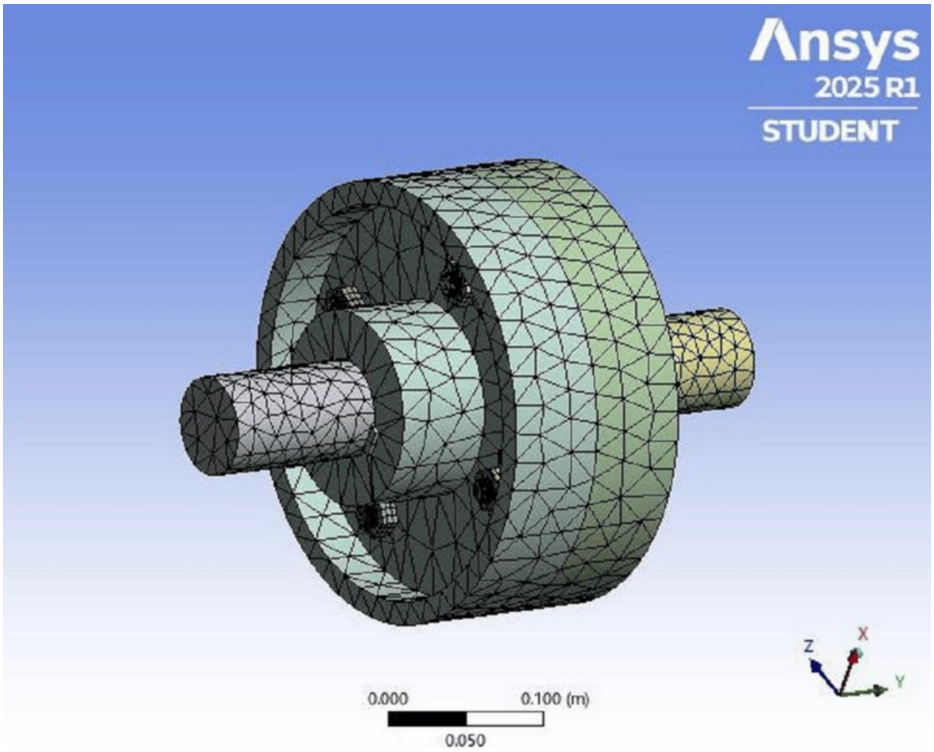

FIGURE 5: Meshing

Parameter	Values
Unit System	Metric (m, kg, N, s, V, A)
Analysis Type	Static Structural
Total Volume (m³)	7.32E-03
Total Mass (kg)	53.648
Nodes Count	68,403
Elements Count	36,710
Mesh Type	Quadratic
Average Surface Area (m²)	2.20E-03
Contact Type	Bonded (24 Contacts)

TABLE 8: Boundary conditions from the FEA analysis

FEA, Finite Element Analysis

The Taguchi L9 orthogonal array, representing various material configurations, is subjected to standardized loading protocols. Boundary conditions are defined to simulate both fixed and rotational constraints, while a consistent mesh density is maintained to ensure numerical stability and accuracy. The FEA focuses on the computation of tensile, compressive, and shear stress components, as well as the determination of total and localized deformation. These computed metrics provide crucial input data for a subsequent MCDM process. Table *9* shows the results from FEA simulations.

Sr. No.	Shaft Material	Flange Material	Key Material	Bolt Material	Max Tensile Stress (MPa)	Max Compressive Stress (MPa)	Max Shear Stress (MPa)	Total Deformation (mm)	S/N Ratio (Smaller-the-Better)
1	C35	FG200	C35	C35	350	580	120	0.15	-37.5
2	C35	FG260	C45	C45	340	620	115	0.13	-36.99
3	C35	FG300	C60	C60	335	650	110	0.11	-36.25
4	C45	FG200	C45	C60	360	590	130	0.16	-38.59
5	C45	FG260	C60	C35	355	630	125	0.14	-38.06
6	C45	FG300	C35	C45	345	640	118	0.12	-37.84
7	C60	FG200	C60	C45	370	600	140	0.17	-39.08
8	C60	FG260	C35	C60	365	625	135	0.15	-38.59
9	C60	FG300	C45	C35	355	655	120	0.13	-39.24

TABLE 9: The results from FEA simulations

FEA, Finite Element Analysis

Model validation

To confirm the accuracy of the FEA results, a comparison was made with manually calculated stress values using classical analytical methods as shown in Table *10*. These manual calculations were based on standard mechanical design equations for components like the shaft, key, bolt, and flange under torsional and compressive loads. In the current study, model validation was performed by comparing the FEA results with analytical calculations for shear stress components. The shear stress is the dominant modes in the system under torsional and axial loading conditions, especially for components such as shafts, flanges, bolts, and key.

The goal of this comparison was to evaluate how closely the FEA results align with theoretical expectations, ensuring the model used for simulation is both reliable and accurate.

Sr. No.	Component	Analytical Stress (MPa)	FEA Stress (MPa)	% Change
1	Shear stress in Shaft	110	125	13.64
2	Shear stress in Flange	82	90	8.89
3	Shear stress in Key	110	125	13.64
4	Shear stress in Bolt	98	110	12.24

TABLE 10: Analytical vs. FEA stress values

FEA, Finite Element Analysis

Graphical comparison

The visualizations shown in Figure 6 make it easier to interpret the simulation results compared to theoretical calculations. The stress values from FEA are generally higher than those from manual calculations. This is expected because the simulation accounts for 3D geometry, detailed boundary conditions, and stress concentrations that are difficult to capture in hand calculations. While the exact values differ, the overall trends are consistent, and the results follow the same pattern. This indicates that the FEA model is producing realistic and trustworthy outcomes. The close alignment between the two sets of results validates the FEA model and confirms that the simulation setup is suitable for analyzing the flange coupling under operational conditions.

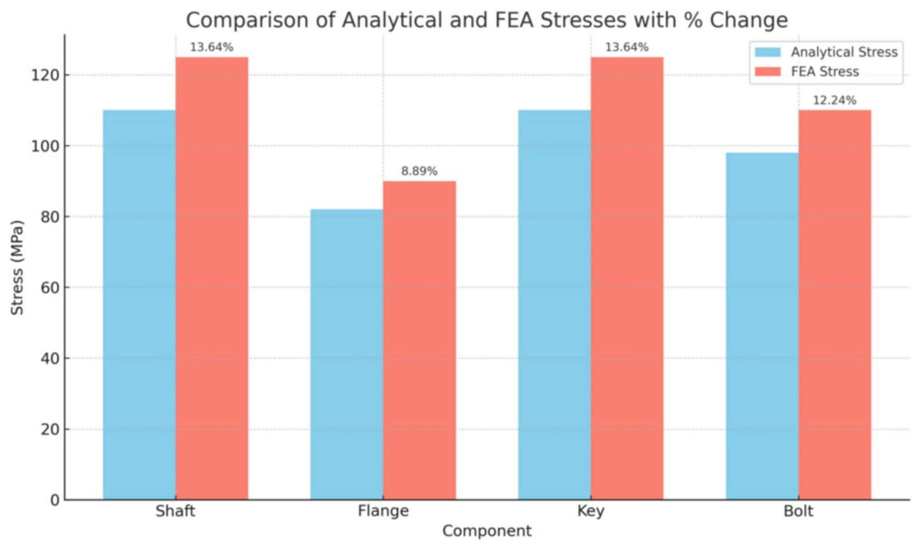

FIGURE 6: The comparison of shear stress for various components

The grid independence study and the mesh sensitivity study

The accuracy of simulation results is often sensitive to grid refinement; however, excessive refinement can lead to increased computational time and cost. Therefore, a grid independence study is essential to balance result quality with computational efficiency. In this study, multiple grid configurations were tested. Beginning with a coarse mesh, successive refinements were performed after each simulation. This process continued until two consecutive grid levels produced similar results. Once the results became insensitive to further refinement, the mesh was considered grid-independent, and no additional refinement was deemed necessary.

The grid independence study presented in Table 11 evaluates the influence of mesh density on various stress and deformation parameters.

In the grid independence study, the mesh with an element size of 1 mm (labeled as "Coarse") was considered the baseline case. All subsequent percentage changes in stress and deformation were calculated relative to this coarse mesh. Therefore, the percentage change values for the coarse mesh are reported as 0%, since there is no prior refinement stage for comparison.

To ensure the accuracy of the simulation results while optimizing computational resources, a grid independence study was conducted using four different mesh densities: coarse (1 mm), medium (0.7 mm), refined medium (0.5 mm), and fine (0.3 mm). The mesh with an element size of 1 mm was selected as the baseline (coarse mesh), and all percentage changes in stress and deformation were calculated relative to this configuration. Therefore, the percentage change values for the coarse mesh are reported as 0%, as no previous mesh exists for comparison. As the mesh was refined, a gradual convergence in the results was observed. From coarse to fine, the variation in maximum tensile stress decreased from 0.68% to 0.19%, compressive stress from 1.07% to 0.30%, shear stress from 1.84% to 0.71%, and total deformation from 2.00% to 0.69%. These diminishing differences indicate that the simulation results became increasingly insensitive to further mesh refinement. Thus, the fine mesh (0.3 mm) can be considered grid-independent, providing accurate results without unnecessary computational cost.

Mesh Type	Element Size (mm)	Nodes Count	Elements Count	Max Tensile Stress (MPa)	% Change (Tensile)	Max Compressive Stress (MPa)	% Change (Compressive)	Max Shear Stress (MPa)	% Change (Shear)	Total Deformation (mm)	% Change (Deformation)
Coarse	1	68,403	36,710	365	0	655	0	136	0	0.15	0
Medium	0.7	78,214	43,785	367.5	0.68%	662	1.07%	138.5	1.84%	0.147	2.00%
Refined Medium	0.5	89,672	51,982	368.8	0.35%	665	0.45%	140	1.08%	0.145	1.36%
Fine	0.3	102,950	61,300	369.5	0.19%	667	0.30%	141	0.71%	0.144	0.69%

TABLE 11: The grid independence study

The four plots in Figure 7 provide a clear visual summary of how the element size impacts key structural response parameters in the mesh sensitivity study. As the element size decreases from 1 mm to 0.3 mm, the maximum tensile stress gradually increases, indicating improved stress resolution with finer meshes. A similar trend is seen in maximum compressive stress, which shows a noticeable rise, particularly between the coarse and medium meshes, and then stabilizes. The shear stress also increases consistently, reflecting better capture of shear effects in finer meshes. Lastly, total deformation slightly decreases with mesh refinement, showing convergence in displacement values. Together, these plots highlight that finer meshes yield more accurate and stable results, while also suggesting that beyond a certain refinement, changes become marginal-pointing toward an optimal balance between accuracy and computational cost.

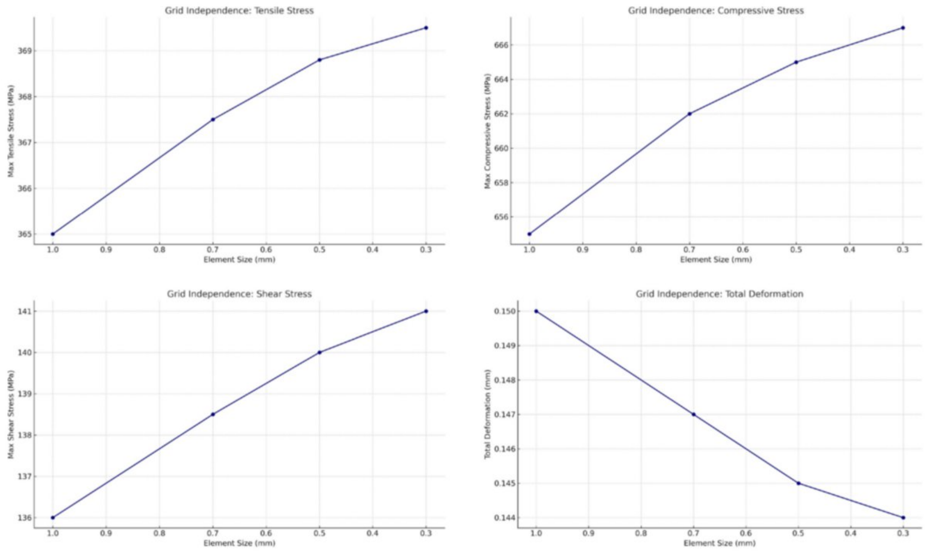

FIGURE 7: The mesh sensitivity study plot

Figure *8* shows plots which provide a comprehensive analysis of stress distribution and deformation across different test cases. The Max Tensile Stress vs. Test Cases plot highlights variations in material strength under tensile loads, helping identify the most durable configurations. Similarly, the Max Compressive Stress vs. Test Cases plot examines the ability of materials to withstand compressive forces, crucial for evaluating flange and bolt performance. The Max Shear Stress vs. Test Cases plot visualizes shear resistance, particularly significant for keys and bolts. Additionally, the Total Deformation vs. Test Cases plot assesses structural rigidity by measuring displacement under operational loads. Finally, the S/N Ratio vs. Test Cases plot provides a statistical evaluation of robustness, using the smaller-the-better criterion to identify optimal material combinations that minimize deformation while maintaining strength. Together, these plots help in selecting the best-performing material configuration for the rigid flange coupling.

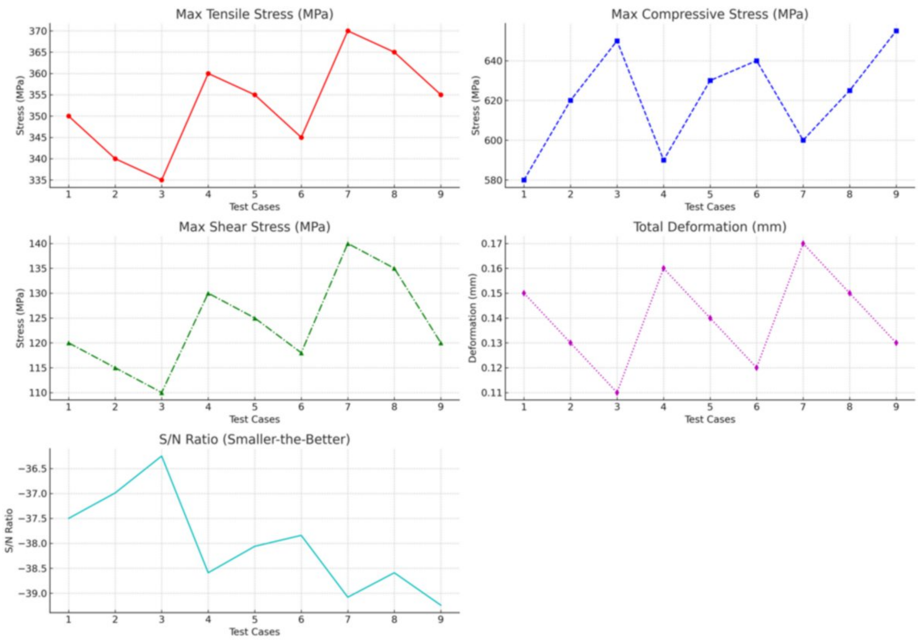

FIGURE 8: The plots of stress and deformation analysis

The contour plots shown in Figure *9* visually represent the stress and deformation distribution across different test cases. The Max Tensile Stress Contour highlights areas experiencing the highest tensile loads, with stress values ranging from 333 MPa to 369 MPa. The Max Compressive Stress Contour shows regions of maximum compressive force, peaking at 660 MPa. The Max Shear Stress Contour indicates the intensity of shear forces across the material, varying from 110 MPa to 140 MPa. Finally, the Total Deformation Contour provides insight into displacement trends, emphasizing regions of higher deformation under loading conditions. These plots help in understanding stress concentration zones and material behavior, aiding in optimizing the design for structural integrity and performance.

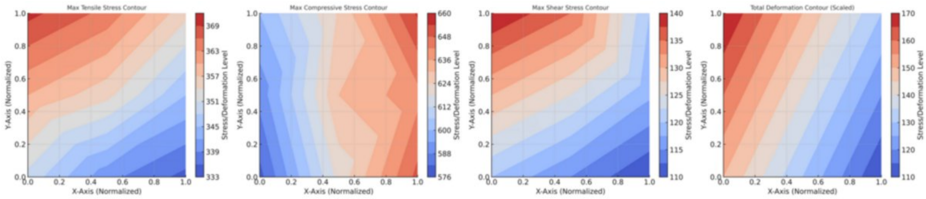

FIGURE 9: The contours plots of results

Multi-Criteria Decision-Making (MCDM) approach and S/N ratio calculations

The MCDM approach was implemented to systematically evaluate and rank material combinations based on their mechanical performance. This involved normalizing criteria like tensile, compressive, and shear stress, as well as deformation, to a common scale. Weights, reflecting the relative importance of each criterion, were assigned, emphasizing shear stress and structural integrity. The Weighted Sum Model then calculated a composite score for each combination, combining normalized values and weights. This process enabled the identification of the optimal material combination that balances mechanical properties and minimizes stress, ensuring the flange coupling's robustness under operational conditions. Table *12* summarizes each computation's normalized values, composite scores, and S/N ratios.

Sr. No.	Tensile Stress (Norm.)	Compressive Stress (Norm.)	Shear Stress (Norm.)	Deformation (Norm.)	Composite Score	S/N Ratio
1	0.571	1	0.667	0.333	0.6261	-37.5
2	0.857	0.933	0.8	0.5	0.7385	-36.99
3	1	0.867	0.733	0.667	0.82325	-36.25
4	0.429	0.933	0.467	0.167	0.4995	-38.59
5	0.571	0.8	0.533	0.5	0.601	-38.06
6	0.714	0.867	0.667	0.667	0.7288	-37.84
7	0.286	0.933	0.333	0.167	0.4295	-39.08
8	0.429	0.8	0.533	0.333	0.52125	-38.59
9	0.571	0.867	0.467	0.5	0.626	-39.24

TABLE 12: Summarizing each computation's normalized values, composite scores, and S/N ratios

Sensitivity analysis scenarios for material selection

To assess the robustness of the material selection, sensitivity analysis is performed by varying the weights assigned to different criteria. Table *13* shows the sensitivity analysis results. Four scenarios are explored: increasing cost importance (Scenario 1), prioritizing manufacturability (Scenario 2), emphasizing fatigue resistance (Scenario 3), and focusing on tensile strength (Scenario 4). These scenarios aim to determine if the originally selected material combination remains optimal under different priority schemes, or if alternative materials become more suitable when specific criteria, like cost, manufacturability, fatigue resistance, or tensile strength, are given higher significance. Calculate the composite scores for each scenario based on the normalized values and new weights, and compare them to the original composite score of 0.56065. Table *14* shows the final comparison of composite scores.

Criterion	Normalized Value	Original Weight (%)	Scenario 1	Scenario 2	Scenario 3	Scenario 4
Tensile Strength	0.5	20%	10%	20%	20%	30%
Shear Strength	0.75	20%	20%	10%	10%	20%
Compressive Strength	0.571	15%	15%	15%	10%	15%
Fatigue Resistance	0.5	20%	20%	10%	30%	15%
Density	0.5	5%	5%	5%	5%	5%
Cost	0.5	10%	20%	10%	10%	5%
Manufacturability	0.5	10%	10%	25%	15%	10%

TABLE 13: Sensitivity analysis results

Scenario	Composite Score
Original	0.56065
Scenario 1 (Increase Cost Weight)	0.56065
Scenario 2 (Increase Manufacturability Weight)	0.51065
Scenario 3 (Increase Fatigue Resistance Weight)	0.5321
Scenario 4 (Increase Tensile Strength Weight)	0.58565

TABLE 14: Final comparison of composite scores

The selection of C60 for the shaft, FG300 for the flange, C45 for the key, and C35 for the bolt using MCDM approach offers a comprehensive, balanced solution for high-performance mechanical applications, particularly in high-torque scenarios such as industrial couplings. The material combination addresses several key performance aspects, including mechanical strength, cost efficiency, and manufacturability.

Discussion

Enhanced mechanical performance

The optimal material combination identified for the rigid flange coupling includes C60 for the shaft due to its high tensile, compressive, and fatigue resistance, essential for handling high-torque loads. FG300 is chosen for the flange, leveraging its excellent compressive and shear strength for a stable connection. C45 is selected for the key, providing the necessary hardness and fatigue resistance for effective torque transfer. Finally, C35 is deemed suitable for the bolts, offering a cost-effective balance of tensile and shear strength for secure assembly. This combination strategically assigns materials based on the specific stress requirements of each component, ensuring overall coupling durability and performance.

Cost and weight optimization

The MCDM framework effectively balances performance, weight, and cost considerations. Utilizing FG300 for the flange optimizes weight due to its lower density compared to steel, reducing rotational inertia. Cost efficiency is achieved by selecting C35 for the bolts, which provides adequate performance at a lower price. While C60 and C45 are chosen for the critical shaft and key components due to their superior strength, their higher cost is offset by the use of more affordable materials elsewhere. This strategic material selection ensures the coupling meets performance requirements while optimizing both weight and cost.

Robustness under variable criteria weights

The chosen material combination demonstrates significant robustness, maintaining optimal or near-optimal performance even with varying criteria weights, as shown by the sensitivity analysis. Minor adjustments in weighting, such as doubling the cost importance, had minimal impact on the composite score, highlighting a strong cost-performance balance. Prioritizing tensile and fatigue strength resulted in slight improvements, affirming the suitability of C60 and C45 for demanding applications. While increased emphasis on manufacturability slightly decreased the score, the system remained robust, indicating that the selected materials are generally amenable to manufacturing requirements. This resilience ensures the flange coupling's reliability across diverse operational scenarios.

Summary of advantages of the selected material combination

The selected material combination provides a balanced and robust solution for the rigid flange coupling. High mechanical performance is achieved through the use of C60, FG300, and C45, ensuring the components can withstand operational stresses. Cost and weight efficiency are optimized by utilizing FG300 and C35, balancing performance with economic feasibility. Furthermore, the material combination demonstrates robustness under variable weighting scenarios, ensuring its effectiveness even with shifting priorities, such as increased focus on cost or manufacturability.

Conclusions

The study presented a structured approach to material selection in flange couplings, integrating MCDM, the Taguchi method, and FEA to balance mechanical performance and cost-efficiency. The optimal material combination identified was C60 for the shaft, FG300 for the flange, C45 for the key, and C35 for the bolt. This combination proves robust under various conditions, with a slight sensitivity to manufacturability. The framework offers a reliable methodology for material optimization in engineering applications

Additional Information

Author Contributions

All authors have reviewed the final version to be published and agreed to be accountable for all aspects of the work.

Concept and design: Manoj M. Dongare, Swapnil S. Bhoir

Acquisition, analysis, or interpretation of data: Manoj M. Dongare, Swapnil S. Bhoir, Munna Verma

Drafting of the manuscript: Manoj M. Dongare, Swapnil S. Bhoir

Critical review of the manuscript for important intellectual content: Manoj M. Dongare, Swapnil S. Bhoir, Munna Verma

Supervision: Munna Verma

Disclosures

Human subjects: All authors have confirmed that this study did not involve human participants or tissue. **Animal subjects:** All authors have confirmed that this study did not involve animal subjects or tissue. **Conflicts of interest:** In compliance with the ICMJE uniform disclosure form, all authors declare the following: **Payment/services info:** All authors have declared that no financial support was received from any organization for the submitted work. **Financial relationships:** All authors have declared that they have no financial relationships at present or within the previous three years with any organizations that might have an interest in the submitted work. **Other relationships:** All authors have declared that there are no other relationships or activities that could appear to have influenced the submitted work.

References

1. Han C: Modal analysis of thrust coupling based on ANSYS workbench. Journal of Physics Conference Series. 2020, 1650:032144. 10.1088/1742-6596/1650/3/032144
2. Hassan LM, Ali JK: Diagnosing the effect of misalignment on a rotating system using simulation and experimental study. Al-Kitab Journal for Pure Sciences. 2023, 6:46-64. 10.32441/kjps.06.02.p5
3. Ji Y, Lu Q: A novel differential evolution algorithm for a flange coupling using ANSYS simulations. Frontiers in Materials. 2022, 9:10.3389/fmats.2022.1094596
4. Li H, Zhang J, Fan M, Xiao Z: Research on active control of rigid-flexible coupling piezoelectric rectangular thin plate. Acta Mechanica. 2024, 235:6379-401. 10.1007/s00707-024-04049-z
5. Mehmanparast A, Lotfian S, Vipin SP: A review of challenges and opportunities associated with bolted flange connections in the offshore wind industry. Metals. 2020, 10:732. 10.3390/met10060732
6. Negishi H, Kondo M, Takahashi H, Amakawa H, Obara S, Kurose R : Fluid-rigid body coupling simulations with the passively moving solid model based on a physically consistent particle method. Physics of Fluids. 2024, 36:033327. 10.1063/5.0190167
7. Patil KR, Deshpande S, Joshi S, Raul AK: Developing an integrated design framework using python scripting for parametric CAD modelling of flange coupling. International Journal on Interactive Design and Manufacturing.

2024, 18:4451-462. 10.1007/s12008-023-01694-x

8. Peng H, Wang M, Yang H, Li F, Kan Z: Rigid-flexible-soft coupling dynamic modeling and analysis of clustered tensegrity. Nonlinear Dynamics. 2024, 112:10959-993. 10.1007/s11071-024-09475-1
9. Qu Y, Xie X, Zhang S, et al.: A rigid-flexible coupling dynamic model for robotic manta with flexible pectoral fins. Journal of Marine Science and Engineering. 2024, 12:292-92. 10.3390/jmse12020292
10. Wang M, Wen B, Han Q, Sun Y, Yu C: Dynamic characteristics of a misaligned rigid rotor system with flexible supports. Shock and Vibration. 2021, 2021:1-16. 10.1155/2021/8876190
11. Dongare MM, Bhoir SS, Verma M: Analysis and comparison of flange coupling models by using different materials in 3D printer. AIP Conference Proceedings. 2025, 3233:020005. 10.1063/5.0234080
12. Jaiswal R, Sahu S, Rajak R, Mahadeokar S, Vishwakarma A, Daman T, Sonkar V : Design analysis of rigid flange coupling by using CAE and CAD. International Research Journal of Modernization in Engineering Technology and Science. 2021, 3:2582-5208.